Charge transfer in $S^{2+}+H$ collisions at eV collision energies

R. B. Christensen* and W. D. Watson

Departments of Physics and Astronomy, University of Illinois at Urbana-Champaign, Urbana, Illinois 61801

(Received 11 August 1980; revised manuscript received 20 April 1981)

Ab initio molecular-orbital methods are utilized to obtain potential-energy curves and coupling-matrix elements to assess the cross section for the charge transfer $S^{2+}(^3P)+H(1s)\rightarrow S^+ + H^+$ at electron-volt collision energies. Results of quantal, coupled-channel calculations confirm the indications from the positions of the potential-energy curves that the cross section is quite small—less than about 10^{-20} cm^2 at 1 eV.

I. INTRODUCTION

Renewed interest in atomic, charge-transfer collisions has arisen because of their importance in plasma fusion devices and in astrophysical plasmas. The relevant energies—typically $\gtrsim 100$ eV in the laboratory and $\lesssim 1$ eV in astrophysics—are sufficiently different that individual investigations rarely, if ever, provide data for both areas of application. At the low energies of astrophysical relevance, essentially no experimental data are available. Because of the cosmic abundance of hydrogen, charge-transfer collisions involving atomic hydrogen tend to be of primary importance in astrophysics. However, the reactivity of atomic hydrogen increases the experimental difficulties. Efforts to satisfy astrophysical needs have therefore been primarily theoretical in nature.[1]

For collisions involving hydrogen atoms and ions that are three or more times ionized, there ordinarily are a large number of exoergic final states and the transition probability to at least one will be so large that an appreciable total cross section will result. For singly and doubly charged ions, only a few final states are energetically allowed. Total cross sections can then be small[2] and are particularly sensitive to the specific properties of the system in question. Furthermore, in astrophysical environments the charge transfer with hydrogen can be a major neutralization process for heavier ions even when the cross section is relatively small because of the intrinsic slowness of competing processes (especially, radiative captures).

Optical radiation from low ionization states of sulfur atoms—the abundance of which is influenced by the $S^{2+}+H$ charge transfer—is observed and utilized as a diagonistic in various astrophysical contexts.[3] The research here presents a molecular-orbital study of the relevant potential-energy curves (Sec. III) and of the matrix elements (Sec. IV) that characterize the charge-transfer collision in the $S^{2+}+H$ system at low energies. Our purpose in carrying out this research was to answer the qualitative question of whether or not the $S^{2+}-H$ charge-transfer reaction could be an important neutralization mechanism for S^{2+} in astrophysical conditions. This permitted us to use simplifying approximations which give results of sufficient accuracy to answer the qualitative question, but which should not be uncritically used in detailed modeling. Basic elements in the description of charge transfer at low energies are presented in Sec. II. A discussion of the expected magnitude for the cross section at energies of 1–10 eV—the energies that are likely to be of primary astrophysical importance —is then given in Sec. V.

II. FORMULATION OF THE CHARGE-TRANSFER PROBLEM

For low-energy (i.e., electron-volt) collisions, the large difference between the velocities of the nuclei and of the electrons is utilized in the usual manner to effect a separation between the nuclear and electronic properties,

$$\Psi(\vec{R};\vec{r})=\frac{1}{R}\sum_i F_i(\vec{R})\phi_i(\vec{r}), \tag{1}$$

where $\Psi(\vec{R};\vec{r})$ is the total wave function, $F_i(\vec{R})$ is the nuclear wave function associated with the electronic state i, and the $\phi_i(\vec{r})$ are the electronic wave functions of the various states. The internuclear separation is designated by $\vec{R}$, and $\vec{r}$ represents, collectively, the positions of the electrons. The close-coupled scattering equations that describe charge transfer in the body-fixed frame are then, in atomic units,[4]

$$\begin{aligned}[T_N+U_{ii}+L(L+1)/2\mu R^2-E]F_i(R)&\\ =\sum_{j\neq i}\left(\frac{1}{\mu}\left\langle\phi_i\left|\frac{d}{dR}\right|\phi_j\right\rangle\frac{d}{dR}\right.&\\ \left.+\frac{[L(L+1)]^{1/2}}{\mu R^2}\langle\phi_i|iL_y'|\phi_j\rangle-U_{ij}\right)F(R)&.\end{aligned} \tag{2}$$

In the above,

$$T_N=-\frac{1}{2\mu}\frac{d^2}{dR^2},$$

where μ is the reduced nuclear mass, L is the angular momentum quantum number for nuclear motion, E is the total energy of the system, iL'_y is the electronic angular momentum operator along the y' axis (primed coordinates are the body-fixed, electronic coordinates with z' along the internuclear axis), h_e is the electronic Hamiltonian, and

$$U_{ij}=\langle\phi_i|h_e|\phi_j\rangle.$$

As presented in Eq. (2), the various nuclear states $F_i(R)$ are connected by three different types of off-diagonal matrix elements. In actual calculations, the basis functions ϕ_i usually are chosen so that either the U_{ij} $(i\neq j)$ are zero (the "adiabatic" basis) or the matrix elements of d/dR are zero (the "diabatic" basis). The former set of states are the eigenfunctions of the electronic Hamiltonian and are the well-known Born-Oppenheimer states of the quasimolecule. In the adiabatic basis, the matrix element of d/dR causes transitions between states of the same molecular symmetry whereas the matrix element of iL'_y couples states of different molecular symmetry. In the diabatic basis, states of the same molecular symmetry are coupled by the off-diagonal elements of the electronic Hamiltonian. States of different symmetry are again connected by iL'_y. It is, of course, possible in principle to transform between the two basis sets.[5]

An approximate, analytic solution to Eq. (2) for the case when two states can be isolated and when the transition is between states of the same molecular symmetry (as is ordinarily the case at low energies) is due to Landau (1932) and Zener (1932).[6] The Landau-Zener solution frequently is of satisfactory accuracy[7] and in any case provides valuable guidance for finding the states of primary importance. A close pseudocrossing in the adiabatic basis is usually required for an appreciable cross section in low-energy collisions.

III. POTENTIAL-ENERGY CURVES FOR THE SH^{2+} SYSTEM

In the $S^{2+}(3s^2 3p^2\ ^3P)+H\rightarrow S^{+}+H^{+}$ charge transfer, only two states of $S^{+}+H^{+}$ [$S^{+}(3p^3\ ^2D)+H^{+}$ and $S^{+}(3p^3\ ^2P)+H^{+}$] are predicted to have pseudocrossings at internuclear separations greater than $3a_0$, based on the Coulomb approximation for the potential-energy curves in the final state. Previous experience indicates that crossings inside of this distance are unlikely to be favorable at electron volt energies. Both final states are spin doublets so that the quartet coupling of the initial state can be ignored. Furthermore, since only Σ and Π projections of the electronic angular momentum are possible in the initial state and we are neglecting angular coupling, the Δ projection of the $S^{+}(3p^3\ ^2D)+H^{+}$ state will also be ignored. Thus, only the $^2\Sigma$ and $^2\Pi$ states of the SH^{2+} system will be considered.

The wave functions that represent the relevant states of the SH^{2+} system must asymptotically reduce to those of the separated atoms, and therefore must contain equivalent $3p$ electrons on the sulfur ion. The asymptotic forms of these wave functions are (only open-shell orbitals are displayed explicitly)

$$\begin{aligned}
&(1)\ S^{2+}(3p^2\ ^3P)+H(1s\ ^1S):\ (2xy\bar{s}-sx\bar{y}+sy\bar{x})/\sqrt{6},\ ^2P,\\
&(2)\ S^{+}(3p^3\ ^2P)+H^{+}:\ (zx\bar{x}+zy\bar{y})/\sqrt{2},\ ^2P,\\
&(3)\ S^{+}(3p^3\ ^2D)+H^{+}:\ (2xyz-zx\bar{y}+zy\bar{x})/\sqrt{6},\ ^2D,\\
&(4)\ S^{2+}(3p^2\ ^3P)+H(1s\ ^1S):\ (2zx\bar{s}-sz\bar{x}+sx\bar{z})/\sqrt{6},\ ^2P,\\
&(5)\ S^{+}(3p^3\ ^2P)+H:\ (xy\bar{y}+xz\bar{z})/\sqrt{2},\ ^2P,\\
&(6)\ S^{+}(3p^3\ ^2D)+H^{+}:\ (xy\bar{y}-xz\bar{z})/\sqrt{2},\ ^2D,
\end{aligned}\qquad (3)$$

where the convention

$$\Phi_\alpha\Phi_\beta\Phi_\gamma\equiv\det|\Phi_\alpha(1)\Phi_\beta(2)\Phi_\gamma(3)|$$

along with Φ (spin up) and $\bar{\Phi}$ (spin down) are utilized. The spatial orbitals are labeled in terms of their transformation properties under rotations. Because the basis functions used in the available computer codes for molecular quantum mechanics are expressed in terms of Cartesian spherical harmonics, the angular parts of the orbitals are also in terms of Cartesian rather than the usual spherical harmonics. Orbitals x, y, and z correspond to the equivalent $3p$ electrons centered on the sulfur nucleus whereas the s orbital is a $1s$ orbital centered on hydrogen nucelus. The z axis is taken to lie along the internuclear axis.

In order to display the molecular symmetry of the wave functions, we will express the orbitals in terms of their molecular symmetries rather than their atomic symmetries. The atomic x

and y orbitals have π molecular symmetry, whereas the z and s orbitals have σ molecular symmetry. As the internuclear separation decreases, the orbitals asymptotically labeled as s or z can only be characterized as σ orbitals and will in general contain both s and z Gaussian-type basis functions (GTF's). When expressed in terms of orbitals with molecular symmetry, the wave functions take the following forms:

$$
\begin{aligned}
&(1)\ (2\pi_x\pi_y\bar{\sigma}_3 - \sigma_3\pi_x\bar{\pi}_y + \sigma_3\pi_y\bar{\pi}_x)/\sqrt{6},\ {}^2\Sigma^-,\\
&(2)\ (\sigma_2\pi_x\bar{\pi}_x + \sigma_2\pi_y\bar{\pi}_y)/\sqrt{2},\ {}^2\Sigma^+,\\
&(3)\ (2\pi_x\pi_y\bar{\sigma}_2 - \sigma_2\pi_x\bar{\pi}_y + \sigma_2\pi_y\bar{\pi}_x)/\sqrt{6},\ {}^2\Sigma^-,\\
&(4)\ (2\sigma_2\pi_x\bar{\sigma}_3 - \sigma_2\sigma_3\bar{\pi}_x + \sigma_2\pi_x\bar{\sigma}_3)/\sqrt{6},\ {}^2\Pi,\\
&(5)\ (\pi_x\pi_y\bar{\pi}_y + \pi_x\sigma_2\bar{\sigma}_2)/\sqrt{2},\ {}^2\Pi,\\
&(6)\ (\pi_x\pi_y\bar{\pi}_y - \pi_x\sigma_2\bar{\sigma}_2)/\sqrt{2},\ {}^2\Pi.
\end{aligned}
\tag{4}
$$

Asymptotically, the σ_2, σ_3, π_x, and π_y orbitals become the z, s, x, and y orbitals, respectively, whereas the σ_1 orbital becomes the sulfur $3s$ orbital.

It should be noted that as a result of symmetry considerations the matrix elements relevant here for charge transfer—those of the electronic Hamiltonian h_e and of the d/dR operator in the approximation that angular coupling can be ignored—can immediately be seen to vanish between certain pairs of states. These operators are nonzero only between states of the same parity and of the same projected angular momentum. Thus, states 1 and 3 and the set of states 4 through 6 can be treated separately. State 2 can be neglected.

A. The $^2\Sigma^-$ states

Examination of the wave functions for states 1 and 3 shows that they differ only in having different σ orbitals. This immediately suggests that the lower state can be found using a Hartree-Fock approach and that the upper state can then be constructed using one of the virtual orbitals from the lower state calculation. The orbitals are expanded in terms of GTF's. Those GTF's centered on the sulfur nucleus are based on the (14s10p) basis set of Huzinaga and Arnaus.[8] The outer three GTF's of the s type were replaced by an equivalent set with more evenly distributed exponents. In addition, two diffuse s-type functions and one diffuse p-type function were added to the basis set along with a set of d-type polarization functions having exponents of 0.54. On the basis of trial calculations for S^{2+}, the resulting (16s11p1d) sulfur basis set was contracted to an (11s7p1d) set. The more diffuse GTF's were left uncontracted so that the basis set would be sufficiently flexible at large internuclear separations to describe the system accurately. For the H1s orbital, a 4s set[9] was used; for the H2p orbital a 3p set[10] was utilized.

Restricted Hartree-Fock (RHF) calculations were performed for state 1 at 18 internuclear separations. The energy of state 3 at these separations was obtained by using the virtual orbitals. Results of this calculation are given in Table I and Fig. 1.

The calculated, asymptotic energy difference between the two states is 0.278 hartrees or 5.1% less than the experimental value of 0.293 hartrees. Were the Coulomb repulsion in the final state to dominate the behavior of the system up to the pseudocrossing, the predicted internuclear separation of the pseudocrossing would be $3.6a_0$.

B. The $^2\Pi$ states

1. General

There are three states of $^2\Pi$ symmetry to be considered. Unfortunately, no technique as simple as the virtual orbital approach used for the $^2\Sigma^-$ states exists for obtaining the energies and wave functions of the upper two states from that of the lower state. The relevant three wave functions cannot be obtained from one another by the simple replacement of a single spatial orbital without altering the spin coupling. Another difficulty is revealed by examining wave functions 5 and 6 [see Eqs. (4)]. In order for them to asymptotically have the appropriate atomic symmetry, the coefficients of the $\pi_x\pi_y\bar{\pi}_y$ and $\pi_x\sigma_2\bar{\sigma}_2$ factors must have equal magnitudes. However, each of these factors is separately a valid $^2\Pi$ molecular con-

TABLE I. SH^{2+}: $^2\Sigma^-$ potential-energy curves.

R (a_0)	State 3 (H)	State 1 (H)	ΔE (H)
99.00	−397.0657	−396.7980	0.2677
10.00	−396.9761	−396.7983	0.1778
8.00	−396.9519	−396.7987	0.1531
7.50	−396.9440	−396.7987	0.1453
7.00	−396.9352	−396.7984	0.1367
6.50	−396.9254	−396.7975	0.1279
6.20	−396.9191	−396.7964	0.1227
5.70	−396.9086	−396.7929	0.1157
5.20	−396.8991	−396.7846	0.1145
4.95	−396.8955	−396.7766	0.1110
4.70	−396.8930	−396.7639	0.1291
4.45	−396.8914	−396.7453	0.1461
4.20	−396.8906	−396.7200	0.1706
3.95	−396.8900	−396.6874	0.2026
3.70	−396.8888	−396.6464	0.2424
3.45	−396.8862	−396.5957	0.2905
3.00	−396.8720	−396.4743	0.3977
2.75	−396.8540	−396.3873	0.4700

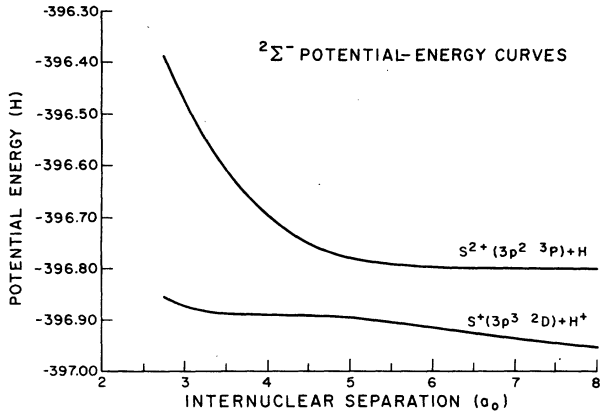

FIG. 1. The calculated $^2\Sigma^-$ adiabatic potential-energy curves for the SH^{2+} system.

figuration and there is no reason to assume that the coefficients of these two configurations in the wave functions of the two lower states should be of equal magnitude at finite internuclear separations. A simple Hartree-Fock approach, in which these coefficients must be specified as input, will then clearly be inadequate. A more sophisticated type of self-consistent field approach, the multiconfiguration self-consistent-field method, in which the coefficients of several configurations are variationally optimized simultaneously with the relevant orbitals, is possible. However, it optimizes only the $^2\Pi$ state of lowest energy. This difficulty in obtaining the wave functions for several states of the same symmetry is inherent in a Hartree-Fock approach because it is based on a variational procedure that gives the lowest energy wave function for a specified spatial and spin symmetry.

As is well known, the configuration-interaction (CI) method can provide approximations to several states of a given symmetry. It was thus decided to utilize the CI approach to obtain the wave functions and potential energy curves for the $^2\Pi$ states.

The major inadequacy in an RHF treatment of the SH^{2+} system is the impossibility of describing the two lower states at finite internuclear separations by $^2\Pi$ configurations that retain their asymptotic form. In a first approximation, this can be remedied by performing a CI calculation including only the three $^2\Pi$ type configurations $-(2\sigma_2\pi_x\bar{\sigma}_3 - \sigma_2\bar{\pi}_x\sigma_3 - \bar{\sigma}_2\pi_x\sigma_3)/\sqrt{6}$, $\pi_x\pi_y\bar{\pi}_y$, and $\pi_x\sigma_2\bar{\sigma}_2$. However, this simple approach neglects the facts that the optimum orbitals for the three different states will not be identical. That is, a set of orbitals capable of describing the lower state well is likely to describe the upper states poorly and vice versa.

2. Orbital corrections

Orbital corrections can be included by adding configurations that allow for orbital mixing and distortion to the three already mentioned. The problem then becomes one of deciding what types of configurations are needed to accurately and equivalently represent all three states.

The initial steps in the selection process are based on physical considerations. A set of occupied and virtual orbitals from the $^2\Sigma^-$ calculation is already at hand. Since the asymptotic forms of the corresponding pairs of $^2\Sigma^-$ and $^2\Pi$ states (i.e., states 1 and 4, and 3 and 6) represent atomic states differing only in magnetic quantum number, the occupied orbitals found in the $^2\Sigma^-$ calculation should be asymptotically accurate for the corresponding $^2\Pi$ states. These orbitals should also be asymptotically good for state 5 since it differs from state 6 only in the way of the sulfur $3p$ orbitals are coupled together. Furthermore, the orbitals inside the $3s$ shell should be quite similar for both the $^2\Sigma^-$ and $^2\Pi$ states at all of the internuclear separations of interest. Their forms are determined largely by the field of the sulfur nucleus and of the other electrons inside the $3s$ shell, and are relatively insensitive to the shape of the outer orbitals.

In contrast, the forms of the σ_1, σ_2, σ_3, π_x, and π_y orbitals can be expected to change significantly in going from the $^2\Sigma^-$ to the $^2\Pi$ case. Certain orbitals are sensitive to the location of the pseudocrossing (i.e., the σ_2 and σ_3 orbitals) and the pseudocrossing for the $^2\Sigma^-$ system occurs at a different internuclear separation from that expected for the $^2\Pi$ system. Even neglecting the shift in the position of the pseudocrossing, the optimum orbitals for the $^2\Sigma^-$ case should differ from those of the $^2\Pi$ case because of the different nature of the charge transfer in the two states. Charge transfer in the $^2\Sigma^-$ system corresponds to a simple one-electron replacement process, whereas in the $^2\Pi$ state it is likely to result from a combination of orbital changes and configuration mixing. Orthogonality constraints between orbitals of the same symmetry type indicate that the σ_1 orbital may be the next most affected orbital, depending on the extent to which the σ_2 and σ_3 orbitals that are optimal for the $^2\Pi$ case incorporate the σ_1 orbital from the $^2\Sigma^-$ case. Unlike the σ orbitals, the π orbitals are not directly involved in the $^2\Sigma^-$ pseudocrossing. Hence the optimum π orbitals will probably change least in going from the $^2\Sigma^-$ to the $^2\Pi$ system.

Although the optimum orbitals for the $^2\Sigma^-$ and $^2\Pi$ systems will differ, to a large extent the $^2\Sigma^-$ orbitals span the energetically favorable regions.

Thus most of the required change in orbital shape can be accounted for in a CI calculation by including those configurations of $^2\Pi$ symmetry generated by making all possible valence orbital substitutions in the three configurations noted above. This set of 18 configurations, listed in Table II, allows for mixing between the valence orbitals and also includes so-called "degeneracy" configurations obtained by replacing orbitals of one symmetry type by orbitals of another symmetry type with similar energies (e.g., $\sigma_1\bar{\sigma}_1\sigma_2\bar{\sigma}_2\pi_x \rightarrow \sigma_2\bar{\sigma}_2\pi_y\bar{\pi}_y\pi_x$). The inclusion of the "degeneracy" configurations should result in wave functions and energies that are somewhat more accurate than those obtained by RHF calculations.

A CI calculation including the 18 configurations mentioned above permits the selection of those configurations which are most important in the description of the $^2\Pi$ states. An important, or dominant, configuration is defined for this purpose as one that has a coefficient greater than or equal to 0.3 at one or more of the internuclear separations at which the CI calculations were performed (to reduce the computational labor, the number of points at which the CI calculations were carried out is less than the number for the RHF calculation of the $^2\Sigma^-$ state). The five configurations that meet this importance criterion (see Table II) account for the bulk of the orbital distortion.

To this point, the possibility of orbital adjustments involving the space spanned by the virtual orbitals has been neglected because these adjustments are expected to be quite small relative to those resulting from mixing of the valence orbitals. However, they must be included in some manner to obtain an accurate wave function.

In order to incorporate into our CI wave function those parts of the orbital corrections that are due to the virtual orbitals, we also include single-excitation configurations (SEC) in the CI calculation. In the SEC, one of the $\sigma_1 \cdots \pi_y$ orbitals in a dominant configuration is replaced by a virtual orbital. This approach is similar in spirit to one used by Schwenzer *et al.*,[11] to obtain RHF quality wave function for several states of the same symmetry. In their calculation, each state was well represented by a single configuration. Thus a good quality wave function for each state consisted of the dominant single configuration plus small "first-order" corrections corresponding to mixing between the occupied orbitals in the dominant configuration and the set of unoccupied, or virtual, orbitals. These wave functions were obtained by carrying out a CI calculation that included the dominant configurations plus the symmetry-restricted, single-excitation configurations (SRSEC) associated with each of the dominant configurations. The SRSEC, defined by Yarkony *et al.*,[12] represent first-order variations of the parent configuration due to small variations in the orbitals that are constrained to satisfy the symmetry and equivalence restriction imposed on an RHF wave function. Thus, Schwenzer *et al.*[11] were able to obtain RHF-type wave functions from a CI calculation.

In adapting the foregoing technique to the calculation of the $^2\Pi$ states, we include the SEC from the five dominant configurations (see Table II) that correspond to: (i) $\sigma_2 \rightarrow \sigma_v$ and $\sigma_3 \rightarrow \sigma_v$ in configurations 3 and 4; (ii) $\pi_x \rightarrow \pi_{xv}$ in configurations 1, 3, 4, and 16; (iii) $\pi^3 \rightarrow \pi^2\pi_v$ in configuration 2; and (iv) $\sigma_1 \rightarrow \sigma_v$ in configurations 1–4 and 16 (the SEC corresponding to $\sigma_2 \rightarrow \sigma_v$ in configuration 1 and to $\sigma^3 \rightarrow \sigma_v$ in configuration 16 are linear combinations of those in group 1). These SEC are then included in a CI calculation with the 18 configurations needed to describe the mixing between the σ_1, σ_2, σ_3, π_x, and π_y orbitals. The resulting wave functions then allow for mixing between the $\sigma_1 \cdots \pi_y$ orbitals and also include the first-order corrections to the $\sigma_1 \cdots \pi_y$ orbitals in the five dominant configurations (see Table III).

TABLE II. SH^{2+} valence-orbital substitution configurations.

(1)	$\sigma_1\bar{\sigma}_1\sigma_2\bar{\sigma}_2\pi_x$ [a]	
(2)	$\sigma_1\bar{\sigma}_1\pi_y\bar{\pi}_y\pi_x$ [a]	
(3)	$\sigma_1\bar{\sigma}_1(\sigma_2\pi_x\sigma_3\theta_1)$ [a]	
(4)	$\sigma_1\bar{\sigma}_1(\sigma_2\pi_x\sigma_3\theta_2)$ [a]	
(5)	$\sigma_2\bar{\sigma}_2\pi_y\bar{\pi}_y\pi_x$	
(6)	$\pi_y\bar{\pi}_y(\sigma_1\pi_x\sigma_2\theta_1)$	
(7)	$\pi_y\bar{\pi}_y(\sigma_1\pi_x\sigma_2\theta_2)$	
(8)	$\pi_y\bar{\pi}_y(\sigma_2\pi_x\sigma_3\theta_1)$	θ_1 and θ_2 are doublet spin functions:
(9)	$\pi_y\bar{\pi}_y(\sigma_2\pi_x\sigma_3\theta_2)$	$\theta_1 = (2\alpha\alpha\beta - \alpha\beta\alpha - \beta\alpha\alpha)/\sqrt{6}$,
(10)	$\sigma_2\bar{\sigma}_2(\sigma_1\pi_x\sigma_3\theta_1)$	$\theta_2 = (\alpha\beta\alpha - \beta\alpha\alpha)/\sqrt{2}$.
(11)	$\sigma_2\bar{\sigma}_2(\sigma_1\pi_x\sigma_3\theta_2)$	
(12)	$\sigma_3\bar{\sigma}_3(\sigma_1\pi_x\sigma_2\theta_1)$	
(13)	$\sigma_3\bar{\sigma}_3(\sigma_1\pi_x\sigma_2\theta_2)$	
(14)	$\pi_y\pi_y(\sigma_1\pi_x\sigma_3\theta_1)$	
(15)	$\pi_y\pi_y(\sigma_1\pi_x\sigma_3\theta_2)$	
(16)	$\sigma_1\bar{\sigma}_1\sigma_3\bar{\sigma}_3\pi_x$ [a]	
(17)	$\sigma_2\bar{\sigma}_2\sigma_3\bar{\sigma}_3\pi_x$	
(18)	$\sigma_3\bar{\sigma}_3\pi_y\bar{\pi}_y\pi_x$	

[a] These are the five most important configurations.

3. *Calculational details*

Because of computational limitations, it was not possible to include the single-excitation configurations corresponding to mixing with all of the virtual orbitals. Accordingly, at each point CI calculations were performed in which the 18 σ_1-π_y mixing configurations were included with the SEC corresponding either to all of the π_x and π_y type

TABLE III. SH^{2+} valence-orbital substitution configurations. The first 18 configurations are those presented in Table II. The remainder are given here.

	Configuration numbers
$\sigma_1\bar{\sigma}_1(\sigma_v\pi_x\sigma_3\theta_1)$	19–34
$\sigma_1\bar{\sigma}_1(\sigma_v\pi_x\sigma_3\theta_2)$	
$\sigma_1\bar{\sigma}_1(\sigma_2\pi_x\sigma_v\theta_1)$	35–50
$\sigma_1\bar{\sigma}_1(\sigma_2\pi_x\sigma_v\theta_2)$	
$\sigma_1\bar{\sigma}_1(\pi_{xv}\sigma_2\bar{\sigma}_2$	51–54
$\sigma_1\bar{\sigma}_1(\pi_x\bar{\pi}_x+\pi_y\bar{\pi}_y)\pi_{xv}/\sqrt{2}$	
$\sigma_1\bar{\sigma}_1[(\pi_x\bar{\pi}_x-\pi_y\bar{\pi}_y)\pi_{xv}+(\pi_x\bar{\pi}_y-\pi_y\bar{\pi}_x)\pi_{yv}]/\sqrt{2}$	55–66
$\sigma_1\bar{\sigma}_1(\pi_x\pi_y\pi_{yv}\theta_1)$	
$\sigma_1\bar{\sigma}_1(\sigma_2\pi_{xv}\sigma_3\theta_1)$	67–74
$\sigma_1\bar{\sigma}_1(\sigma_2\pi_{xv}\sigma_3\theta_2)$	
$(\sigma_v\pi_x\sigma_2\bar{\sigma}_1\bar{\sigma}_2+\sigma_1\pi_x\sigma_2\bar{\sigma}_v\bar{\sigma}_2)/\sqrt{2}$	75–82
$(\sigma_v\pi_x\pi_y\bar{\sigma}_1\bar{\sigma}_3+2\sigma_1\sigma_2\pi_x\bar{\sigma}_v\bar{\sigma}_3+\sigma_v\sigma_2\sigma_3\bar{\sigma}_1\bar{\pi}_x$	
$+\sigma_1\sigma_2\sigma_3\bar{\sigma}_v\bar{\pi}_x-\sigma_v\pi_x\sigma_3\bar{\sigma}_1\bar{\sigma}_2-\sigma_1\pi_x\sigma_3\bar{\sigma}_v\bar{\sigma}_2)/12$	91–105
$(\sigma_v\sigma_2\sigma_3\bar{\sigma}_1\bar{\pi}_x+\sigma_1\sigma_2\sigma_3\bar{\sigma}_v\bar{\pi}_x+\sigma_v\pi_x\sigma_3\bar{\sigma}_1\bar{\sigma}_2+\sigma_1\pi_x\sigma_3\sigma_v\sigma_2)/2$	
$\sigma_1\bar{\sigma}_1\pi_{xv}\sigma_3\bar{\sigma}_3$	107–110
$(\sigma_1\bar{\sigma}_v\pi_x\sigma_3\bar{\sigma}_3+\sigma_v\sigma_1\pi_x\sigma_3\bar{\sigma}_3)/\sqrt{2}$	111–118

virtuals or to all of the σ-type virtuals, excepting the highest energy σ-type virtual. Trial calculations showed that this exception had no noticeable effect on the final energies and wave functions. From the resulting wave functions, the virtuals were ranked in descending order of importance by examining the sum of the squares of the coefficients for the different configurations containing each of the various virtuals. If the ordering resulting from the three different states differed, the order chosen was that of the state in which the SEC of the orbitals in question were most important.

It was desirable to include as many σ-type virtuals as possible since they are expected to suffer the most distortion. Thus no more π_x- and π_y-type virtuals were included than was necessary. Examination of these wave functions at the different internuclear separations showed that four π_x and π_y virtuals were sufficient to describe the bulk of the first-order corrections to π symmetry orbitals. It was then possible to use eight σ-type virtuals to describe the first-order corrections to the σ symmetry orbitals. Hence, at each point the SEC corresponding to mixing between the $\sigma_1\cdots\pi_y$ valence orbitals, the eight most important π virtuals (four π_x and four π_y), and the eight most important σ virtuals are included.

Success with the above approach depends upon having good wave functions in lowest order. The sum of the squares of the coefficients for the five configurations from which the SEC are generated has a minimum of 0.877 (occurring in the second lowest $^2\Pi$ state at $R = 2.75a_0$), and is about 0.96 when averaged over the computed points. Most of the rest of each wave function is accounted for by the remainder of the 18 $\sigma_1\cdots\pi_y$ mixing configurations. The coefficients of the SEC are 0.08 or less. These results tend to indicate that the first-order treatment of the corrections is adequate.

As a further test, CI calculations were performed using orbitals obtained from RHF calculations of the upper $^2\Pi$ state at internuclear separations of $3.95a_0$ and $99a_0$. Because these orbitals are significantly different from those obtained in the RHF calculation of the $^2\Sigma^-$ ground state, any inadequacy in the treatment of the orbital adjustment should be evident in the form of significant differences in the energies of the corresponding states. Even more important from the standpoint of the charge-transfer problem are the energy separations between the initial (upper) state and the two lower states.

The same selection procedures described previously were applied to the configurations which where constructed from the $^2\Pi$ orbitals. In addition, the SEC corresponding to the least important of the five dominant configurations were included even though the coefficient of this configuration was less than 0.3 at $3.95a_0$ and $99a_0$. This was done for consistency since these configurations were included in the CI calculations which used the $^2\Sigma^-$ orbitals. Although the coefficients of corresponding configurations in the wave functions are quite different, as expected, the five dominant configurations are the same for both sets of calculations.

The results of the CI calculations based on the

RHF orbitals for the $^2\Pi$ state are compared in Table IV with the results obtained using the $^2\Sigma^-$ orbitals. Between any two corresponding states, the maximum energy difference is 0.14 eV, which occurs for the lowest state at $99a_0$. The maximum percentage change in the excitation energies between any pair of states is 6% and arises in the energy difference between the two lowest states at $99a_0$. At $3.95a_0$, the maximum percentage difference in the excitation energies is 0.88%, also for the energy difference between the two lowest states. The percentage differences in the energy separations between the upper state and the two lower states, which are of greater importance when considering the charge-transfer problem, range from 1.7% for states 4 and 5 at $99a_0$ to 0.56% for states 4 and 6 at $3.95a_0$. These results indicate that sufficient flexibility has been incorporated into the wave functions to attain the accuracy needed for our purposes. The full potential-energy curves obtained for the $^2\Pi$ states by using the procedures described above are presented in Fig. 2.

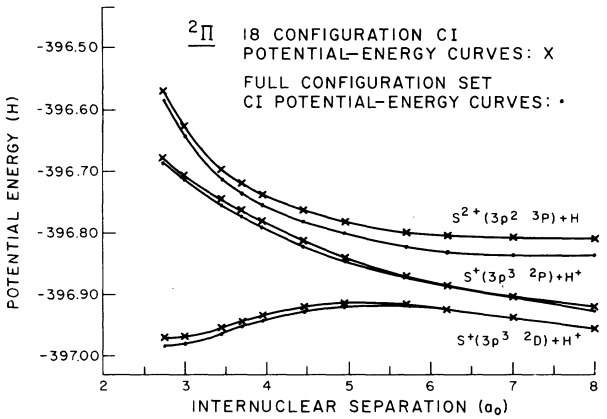

FIG. 2. The $^2\Pi$ adiabatic potential-energy curves for the SH^{2+} system calculated using the CI approximation with the 18-valence-orbital configurations (×), and with these 18 configurations plus the virtual-orbital mixing configuration (●).

IV. CALCULATION OF THE INTERACTION MATRIX ELEMENTS FOR CHARGE TRANSFER

A. The $^2\Sigma^-$ states

Because of the large difference in energy between the two $^2\Sigma^-$ states, we expect that the cross section for this channel will be effectively zero at the energies of primary interest ($\simeq$1 eV). In any case it should be much smaller than the cross section in the $^2\Pi$ channel. Nevertheless, a knowledge of the $\langle\sigma_2|d/dR|\sigma_3\rangle$ matrix element obtained from the interaction in the $^2\Sigma^-$ state will be useful in consideration of the $^2\Pi$ channels.

Instead of calculating explicitly the adiabatic matrix element for radial coupling, an approximate technique is utilized that is based on expansions in a Taylor series about the diabatic crossing point.[13] In this procedure the radial coupling term between states i and j can, to lowest order, be parametrized by

$$\left\langle i\left|\frac{d}{dR}\right|j\right\rangle = \frac{-\alpha}{[2\alpha(R-R_x)+\gamma]^2+1}, \tag{5}$$

where the parameters α, γ, and R_x are determined by the properties of the (as yet undetermined) diabatic states at the crossing point. The transformation matrix from adiabatic to diabatic states can then be obtained from the integral of the radial coupling term

$$\theta(R) = \int_{\infty}^{R} \left\langle i\left|\frac{d}{dR}\right|j\right\rangle dR\,. \tag{6}$$

Using the calculated curves for the energies of the adiabatic states and the above form for $\theta(R)$, we vary α and γ until smooth diabatic curves are generated. An additional criterion used to differentiate between pairs of α and γ that give similarly smooth diabats is the smoothness of the approximate, diabatic U_{12} through the crossing region. The optimum values so obtained are $\alpha = 0.382$ and $\gamma = 0.19$. In Figs. 3 and 4, we present the diabatic curves and the $U_{12}(R)$ corresponding to this choice of parameters.

Though somewhat different in detail, the above approach is similar in spirit to that used by others[14] in that approximate curve fitting is used to find diabatic states. While such approaches clearly are not as accurate as a direct numerical calculation of the matrix elements, they do provide a basis on which to assess the likely importance of radial coupling for the $^2\Pi$ system. A more accurate (and laborious) calculation could, if warranted, then be performed.

TABLE IV. Comparison between $^2\Sigma^-$ and $^2\Pi$ orbital sets.

	$^2\Sigma^-$ Orbital set	$^2\Pi$ Orbital set
	$R = 3.95a_0$	
state 6 (H)	−396.9424	−396.9451
state 5 (H)	−396.7900	−396.7913
state 4 (H)	−396.7525	−396.7541
	$R = 99a_0$	
state 6 (H)	−397.0658	−397.0691
state 5 (H)	−397.0350	−397.0402
state 4 (H)	−396.8348	−396.8366

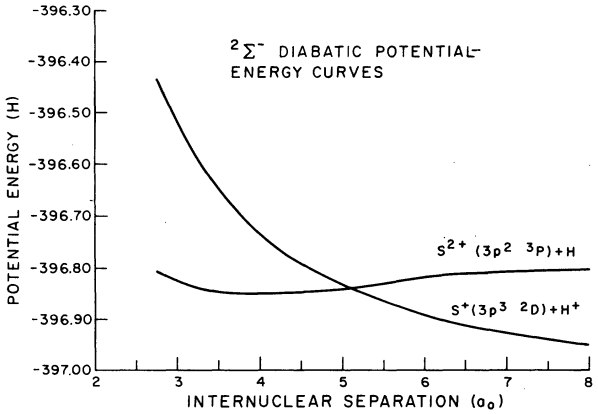

FIG. 3. The $^2\Sigma^-$ diabatic potential-energy curves for the SH^{2+} system derived from the adiabatic potential-energy curves using the approximate diabatic interaction matrix element shown in Fig. 4.

B. The $^2\Pi$ states

Interpretation of the $^2\Pi$ potential-energy curves is complicated by the presence of bonding effects. In particular, with decreasing internuclear separation the energies of the asymptotically degenerate configurations $\pi_x\pi_y\bar{\pi}_y$ and $\pi_x\sigma_2\bar{\sigma}_2$ [see Eq. (4)] begin to diverge as a result of the differing susceptibility of the $\pi_y\bar{\pi}_y$ and $\sigma_2\bar{\sigma}_2$ groups to bonding effects. The latter group, being directed along the internuclear axis, tends to form a two-electron bond with the proton. In contrast, the $\pi_y\bar{\pi}_y$ group, being directed perpendicular to the internuclear axis, does not show appreciable bonding effects. Thus as internuclear separation decreases, the $\pi_x\pi_y\bar{\pi}_y$ configuration becomes increasingly important in state 5, whereas the $\pi_x\sigma_2\bar{\sigma}_2$ configuration decreases in importance. The opposite trend is apparent in state 6. This suggests that the presence of a minimum in the energy separation between states 4 and 6 at an internuclear separation of $6.1a_0$ is most probably due to bonding effects rather than to a pseudocrossing. In any case, the energy separation between this pair of states is so large as to make it very unlikely that their interaction provides a significant contribution to the cross section for charge transfer.

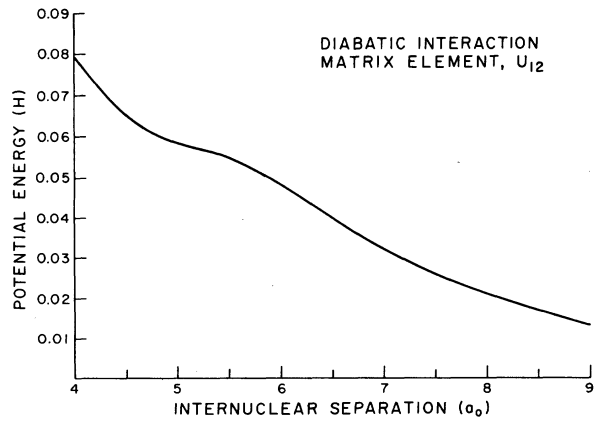

FIG. 4. The approximate diabatic interaction matrix element determined from the calculated adiabatic potential-energy curves for the $^2\Sigma^-$ state of the SH^{2+} system.

At an internuclear separation of $3.9a_0$, there is a minimum in the energy difference between states 4 and 5. Unlike the case above, bonding effects in the lower of these two states plays no role in the occurrence of a minimum in the energy difference. There is no indication of bonding behavior in the potential-energy curves, and in addition, state 5 is dominated by the $\pi_x\pi_y\bar{\pi}_y$ configuration (coefficient $\gtrsim 0.96$) in this region which, as stated previously, is expected to display little bonding behavior.

Furthermore, examination of the relevant wave functions shows no indication of the interchange of character typical of a pseudocrossing. Unlike the situation for states 4 and 6, in which a possible interchange of character would be obscured by the configuration mixing necessitated by orbital adjustment, any interchange of character between states 4 and 5 would be apparent, since state 5 is largely dominated by a single configuration ($\pi_x\pi_y\bar{\pi}_y$) that is relatively unaffected by orbital adjustments. These considerations indicate that the potential-energy curves of states 4 and 5 do not form a pseudocrossing at $3.9a_0$.

Nevertheless, the two states are quite close to each other over an appreciable distance so that a significant contribution from this channel to the charge transfer cannot immediately be excluded. To assess quantitatively the contribution from this channel, the following approximate calculation was performed to obtain the relevant interaction matrix elements. It should be kept in mind that the actual curves have a somewhat larger energy separation than do the computed curves. We will deal with this subsequently.

The calculational method involves finding approximate wave functions for the two states for which we can readily obtain $\langle\psi_A|h|\psi_B\rangle$ and $\langle\psi_A|d/dR|\psi_B\rangle$. This is done by dividing the set of configurations into two mutually exclusive sets and restricting the configurations allowed in the wave functions of each state to one or the other of the two sets. That such might be a reasonable approach is suggested by the fact that the wave functions which correspond to the two states of

interest are dominated by different configurations. The division simplifies the calculation of the interaction matrix element in the following manner.

1. The d/dR matrix element

The matrix element of d/dR between any two CI wave functions ψ_A and ψ_B can be expressed as

$$\left\langle \psi_A \left| \frac{d}{dR} \right| \psi_B \right\rangle = \sum_{i,j} \left(C_{Ai} C'_{Bj} \delta_{ij} + C_{Ai} C_{Bj} \left\langle \phi_i \left| \frac{d}{dR} \right| \phi_j \right\rangle \right), \quad (7)$$

where C_{Ai} and C_{Bi} are the coefficients of the ith configuration ϕ_i in wave functions ψ_A and ψ_B, respectively, and $C_{Bj} = dC_{Bj}/dR$. Because ψ_A and ψ_B are formed from mutually exclusive sets of configurations, the first term on the right-hand side of this equation is eliminated by the action of the delta function. To simplify the evaluation of the second term, all of the configurations that involve virtual orbitals are excluded. A set of 18 configurations remains. The adiabatic potential-energy curves obtained with the 18 configurations alone are compared in Fig. 2 with those found using the full set. As might be expected, the main effect of excluding the configurations with virtual orbitals is to raise the energy of the upper state (state 5).

Within this limitation, large contributions to $\langle \phi_i | d/dR | \phi_j \rangle$ can only come from pairs of configurations ϕ_i and ϕ_j of which one contains the σ_2 orbital and the other, the σ_3 orbital. Then $\langle \phi_i | d/dR | \phi_j \rangle$ will be given approximately by $a_{ij} \langle \sigma_2 | d/dR | \sigma_3 \rangle$, where the a_{ij} are determined from the symmetry restricted coefficients of the various Slater determinants in ϕ_i and ϕ_j. An estimate for $\langle \sigma_2 | d/dR | \sigma_3 \rangle$ was found previously in the discussion of the $^2\Sigma^-$ channel. The function $\langle \psi_A | d/dR | \psi_B \rangle$, which is thus found from Eq. (7), is presented in Fig. 5. If on this basis the contribution of the $\langle d/dR \rangle$ term seems likely to be important, a more detailed calculation for it would be warranted.

2. The U_{ij} matrix element

Fortunately, the computational techniques necessary for evaluating the U_{ij} $(i \neq j)$ matrix elements are similar to those used in the CI program. The first step in the process outlined above is the selection of the configurations to be placed in each of the two sets. To ensure that the wave function of each state is accurately represented both at infinity and at the point of minimum energy separation, the fully adiabatic 18-configuration wave functions at these points were examined and the most important configurations for each state were selected. At infinity, state 4 is dominated by configurations 3 and 8, whereas state 5 is dominated by configurations 1, 2, and 5. At $3.95a_0$, in addition to the configurations already listed, configurations 4 and 16 were important in state 4 while configuration 7 was important in state 5. The sum of the squares of the coefficients of these four most important configurations in each wave function exceeds 0.96 at every point included in the calculation. This implies that wave functions for states 4 and 5 formed from these two disjoint sets of configurations will be reasonable approximations to the actual wave functions. To increase further the accuracy of the wave functions, the remaining 10 configurations were distributed as much as possible to allow for mixing among the σ-type orbitals in the four most important wave functions of each set. The final configuration sets are given in Table V, while the resulting potential energies of the states in this approximation and the interaction matrix elements are shown in Fig. 5. For comparison, $\langle \psi_4 | h_e | \psi_5 \rangle$ calculated with inclusion of the virtual-orbital configurations is also shown. The agreement between the two forms is an indication that the accuracy is satisfactory for the purposes here.

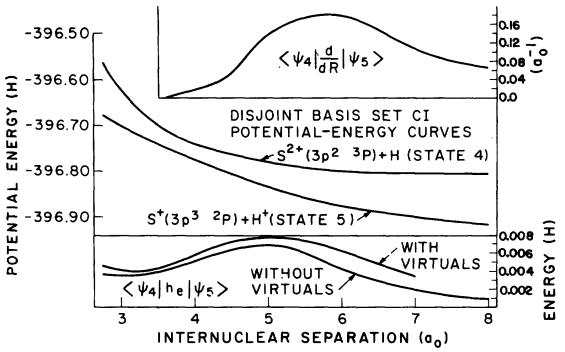

FIG. 5. Potential-energy curves for the $^2\Pi$ states 4 and 5 obtained with the disjoint basis set CI technique. Also shown are the associated adiabatic and diabatic radial, coupling-matrix elements.

V. ESTIMATES FOR THE CROSS SECTION

Since it appears that no curve crossing actually occurs in the $^2\Pi$ channel—the channel that as previously noted would seem to produce the largest contribution—the Landau-Zener approximation is inapplicable. Because the minimum energy separation is in the repulsive region and because a small transition probability is anticipated, the accuracy of the semiclassical treatments of the collision is particularly questionable in this case. Numerical integrations of the quantal scattering

TABLE V. Configurations used in disjoint basis set calculation of U_{45} and $\langle\psi_4|d/dR|\psi_5\rangle$.

Configurations included in state 4
$\sigma_1\bar{\sigma}_1(\sigma_2\pi_x\sigma_3\theta_1)$
$\sigma_1\bar{\sigma}_1(\sigma_2\pi_x\sigma_3\theta_2)$
$\pi_y\bar{\pi}_y(\sigma_2\pi_x\sigma_3\theta_1)$
$\pi_y\bar{\pi}_y(\sigma_2\pi_x\sigma_3\theta_2)$
$\sigma_2\bar{\sigma}_2(\sigma_1\pi_x\sigma_3\theta_1)$
$\sigma_2\bar{\sigma}_2(\sigma_1\pi_x\sigma_3\theta_2)$
$\sigma\ \bar{\sigma}_3(\sigma_1\pi_x\sigma_2\theta_1)$
$\sigma_3\bar{\sigma}_3(\sigma_1\pi_x\sigma_2\theta_2)$
$\sigma_1\bar{\sigma}_1\pi_y\bar{\pi}_y\bar{\pi}_x$
Configurations included in state 5
$\sigma_1\bar{\sigma}_1\sigma_2\bar{\sigma}_2\pi_x$
$\sigma_1\bar{\sigma}_1\pi_y\bar{\pi}_y\pi_x$
$\sigma_2\bar{\sigma}_2\pi_y\bar{\pi}_y\pi_x$
$\pi_y\bar{\pi}_y(\sigma_1\pi_x\sigma_2\theta_1)$
$\pi_y\bar{\pi}_y(\sigma_1\pi_x\sigma_2\theta_2)$
$\pi_y\bar{\pi}_y(\sigma_1\pi_x\sigma_3\theta_1)$
$\pi_y\bar{\pi}_y(\sigma_1\pi_x\sigma_3\theta_2)$
$\sigma_2\bar{\sigma}_2\sigma_3\bar{\sigma}_3\pi_x$
$\sigma_3\bar{\sigma}_3\pi_y\bar{\pi}_y\pi_x$

equations [Eq. (1)] for a collision involving only states 4 and 5 have therefore been performed[15] with data from Fig. 5, and are reproduced in Fig. 6. Three sets of cross sections have been computed: (i) one with coupling between the states from both the U_{45} and d/dR matrix elements, (ii) a second with coupling only through U_{45}, and (iii) finally, a set with coupling only through U_{45} but with the separation in energy of the two states increased by a constant amount to reproduce the experimental asymptotic separation. Comparison of cross sections (i) and (ii) provides an indication of the importance of d/dR coupling with the result that it does not cause a significant increase in the cross section. This tends to support the notion that the states can be treated as diabatic. Shifting diabatic potential-energy curves by a constant amount to reproduce the proper asymptotic energy separation is considered likely to lead to a reasonable estimate for the cross section.[16] The incomplete description of correlation which causes the inaccuracies in total energy ordinarily is not critical for the calculation of U_{45}. Because a diabatic state (in contrast to an adiabatic state) consists largely of orbitals of similar character on both sides of an interaction region, simply shifting the total energy by a constant amount at all internuclear separations is a realistic approximation. The best estimates for the cross sections for $S^{2+}+H$ charge transfer are thus the set (iii).

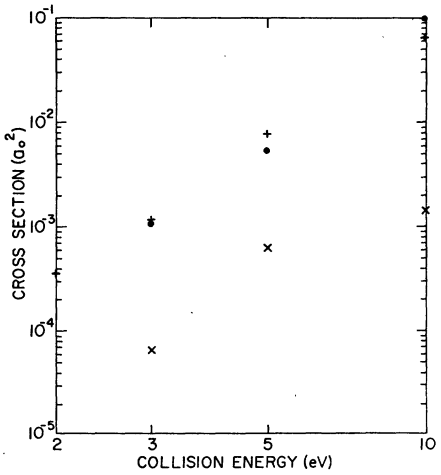

FIG. 6. Cross section for charge transfer involving $^2\Pi$ states 4 and 5 versus center-of-mass translational energy for three cases: calculated potential-energy curves with coupling by the d/dR and U_{45} coupling-matrix elements (+), calculated potential-energy curves with coupling by only the U_{45} coupling-matrix element (•), and potential-energy curves shifted by a constant to reproduce the asymptotic separation with coupling only by the U_{45} coupling-matrix element (×) (from Ref. 15).

Because of the smallness of the cross sections, the computer code was unable to produce reliable cross sections for collision energies below about 3 eV. At energies near 1 eV, which are of primary interest for astrophysical gases, the cross section appropriate for this asymptotically correct pair of energy levels would be well below the value of approximately $10^{-4}a_0^2$ computed at 3 eV. The product of this cross section by the collision speed is then about 10^{-14} cm^{3}s^{-1}—a seemingly conservative upper limit to the rate coefficient at temperatures $T \simeq 10^4$ K.

In our treatment of the charge transfer of SH^{2+} we have assumed that the transition is dominated by radial couplings, and have thus neglected the possible contributions from rotational couplings between the $^2\Sigma^-$ and $^2\Pi$ states. At the relatively low collision energies of interest here, any large cross sections for charge transfer ordinarily are expected to be due to radial coupling because of the velocity dependence of the rotational coupling.

As in the case for radial coupling, transitions with rotational coupling are favored by the presence of a crossing. The noncrossing rule does not apply to states of different symmetry and the relevant potential-energy curves may, in fact, cross. An approximate form for the transition probability that is analogous to the Landau-Zener expression, but for the case of a curve crossing with rotational coupling, is available.[17] This expression provides some guidance. In the SH^{2+} system, there are no such crossings between states of different symmetry. We thus expect that any contribution from rotational coupling will be unimportant in

comparison with that already computed from the radial coupling.

In the absence of a large charge-transfer cross section due to radial or rotational coupling, it is possible that the radiative charge-transfer mechanism described by Butler *et al.*[18] makes a significant contribution to the total cross section. Although we have not calculated the contribution to the S^{2+}-H cross section due to this mechanism, the results of Butler *et al.*[18] suggest that it will be of the same order of magnitude as that due to the radial coupling ($\sim 10^{-14}$ $cm^3 s^{-1}$ at $T \sim 10^4$ K).

It is encouraging to note that this value for the S^{2+}-H charge-transfer reaction rate is consistent with the prediction made by Péquignot *et al.*[3] This prediction was based on the value of the S^{2+}-H charge-transfer reaction rate that was needed to obtain agreement between their model of the ionization structure of the planetary nebula NGC 7027 and observations.

ACKNOWLEDGMENTS

The authors are indebted to a number of people for helpful interactions and for the use of their computer codes during the course of this investigation: R. J. Blint, C. E. Dykstra, A. B. Kunz, and G. T. Surratt. We also thank C. A. Feickert for allowing us to cite his unpublished work. This research has been supported in part by a NSF Grant No. AST78-23648.

---

*Current address: Joint Institute for Laboratory Astrophysics, University of Colorado, Boulder, Colorado 80309.

[1]For example, W. D. Watson, Annu. Rev. Astron. Astrophys. 16, 585 (1978); S. E. Butler, T. G. Heil, and A. Dalgarno, Astrophys. J. 241, 442 (1980).

[2]For example, R. McCarroll and P. Valiron, Astron. Astrophys. 44, 465 (1975).

[3]D. Péquignot, S. M. V. Aldrovandi, and G. Strasinska, Astron. Astrophys. 63, 313 (1978).

[4]W. R. Thorson and J. B. Delos, Phys. Rev. A 18, 117 (1978).

[5]F. T. Smith, Phys. Rev. 179, 111 (1969).

[6]L. Landau, Z. Phys. Sowjet 2, 46 (1932); C. Zener, Proc. R. Soc. London Ser. A 137, 696 (1932).

[7]W. D. Watson and R. B. Christensen, Astrophys. J. 231, 627 (1969).

[8]S. Huzinaga and C. Arnau, J. Chem. Phys. 53, 348 (1970).

[9]T. H. Dunning, J. Chem. Phys. 53, 2873 (1970).

[10]S. Huzinaga, J. Chem. Phys. 42, 1293 (1965).

[11]G. M. Schwenzer, S. V. O'Neil, H. F. Scahefer III, C. P. Baskin, and C. F. Bender, J. Chem. Phys. 60, 2787 (1974).

[12]D. R. Yarkony, H. F. Schaefer III, and C. F. Bender, J. Chem. Phys. 64, 981 (1976).

[13]M. B. Faist and R. D. Levine, J. Chem. Phys. 64, 2953 (1976).

[14]R. McCarroll and P. Valiron, Astron. Astrophys. 53, 83 (1976).

[15]C. Feichert (unpublished).

[16]L. R. Kahn and P. J. Hay, J. Chem. Phys. 61, 3530 (1974); R. J. Blint, W. D. Watson, and R. B. Christensen, Astrophys. J. 205, 634 (1976).

[17]A. Russek, Phys. Rev. A 4, 1918 (1971).

[18]S. E. Butler, S. L. Guberman, and A. Dalgarno, Phys. Rev. A 16, 500 (1977).